Published in final edited form as:
Virology. 2012 January 20; 422(2): 317–325. doi:10.1016/j.virol.2011.10.033.

Adenovirus E4-ORF3-dependent relocalization of TIF1α and TIF1γ relies on access to the Coiled-Coil motif

Elizabeth I. Vink[a], **Mark A. Yondola**[b,1], **Kai Wu**[a], and **Patrick Hearing**[a,*]

[a]Department of Molecular Genetics and Microbiology, School of Medicine, Stony Brook University, Stony Brook, New York 11794

[b]Department of Microbiology, Mount Sinai School of Medicine, One Gustave L. Levy Place, New York, NY 10029

Abstract

The adenovirus E4-ORF3 protein promotes viral replication by relocalizing cellular proteins into nuclear track structures, interfering with potential anti-viral activities. E4-ORF3 targets transcriptional intermediary factor 1 alpha (TIF1α), but not homologous TIF1β. Here, we introduce TIF1γ as a novel E4-ORF3-interacting partner. E4-ORF3 relocalizes endogenous TIF1γ in virus-infected cells *in vivo* and binds to TIF1γ *in vitro*. We used the homologous nature, yet differing binding capabilities, of these proteins to study how E4-ORF3 targets proteins for track localization. We mapped the ability of E4-ORF3 to interact with specific TIF1 subdomains, demonstrating that E4-ORF3 interacts with the Coiled-Coil domains of TIF1α, TIF1β, and TIF1γ, and that the C-terminal half of TIF1β interferes with this interaction. The results of E4-ORF3-directed TIF1 protein relocalization assays performed *in vivo* were verified using coimmunoprecipitation assays *in vitro*. These results suggest that E4-ORF3 targets proteins for relocalization through a loosely homologous sequence dependent on accessibility.

Keywords

Adenovirus; Ad; E4-ORF3; nuclear tracks; relocalization; TIF1α; TIF1γ

Introduction

The Adenovirus (Ad) early region 4 (E4) plays an essential role in promoting a successful virus replication cycle. Loss of the entire E4 region leads to defects in viral DNA replication as well as a reduction in infectious particle production (Halbert, Cutt, and Shenk, 1985; Weinberg and Ketner, 1986). In addition, protein products of the E4 region are required for effective shutoff of host cell protein synthesis, late viral mRNA accumulation, and late protein synthesis (Halbert, Cutt, and Shenk, 1985; Weinberg and Ketner, 1986). Of the six known E4 protein products, reintroduction of either the E4-ORF6 or the E4-ORF3 protein is sufficient to restore virus growth properties to near wild type levels (Bridge and Ketner, 1989; Huang and Hearing, 1989).

*Corresponding author, Fax +1 631 632 8891. phearing@ms.cc.sunysb.edu.
[1]Present address

Together with the Ad E1B-55K protein, the E4-ORF6 protein functions as an adaptor molecule in an E3 cullin-RING ligase complex (Harada et al., 2002; Querido et al., 2001), promoting the ubiquitination and proteosome-dependent degradation of substrates such as p53 (Harada et al., 2002; Querido et al., 2001), Mre11-Rad50-Nbs1 (MRN) complex proteins (Stracker, Carson, and Weitzman, 2002), DNA ligase IV (Baker et al., 2007), integrin α3 (Dallaire et al., 2009), and bloom helicase (Orazio et al., 2010). In addition to targeting known substrate proteins, the E4-ORF6 and E1B-55K ubiquitin ligase complex also facilitates the nuclear export of viral mRNA (Blanchette et al., 2008; Woo and Berk, 2007). Independent of the E1B-55K interaction, the E4-ORF6 protein is able to bind p53, blocking its downstream transcriptional activities (Dobner et al., 1996).

The E4-ORF3 and E4-ORF6 proteins inhibit an overlapping, but non-identical, pool of target cellular proteins. Rather than targeting proteins for degradation, E4-ORF3 promotes a productive infection by recruiting cellular proteins into elongated nuclear track structures, inhibiting their anti-viral properties. This is evident in the disparate mechanisms by which both E4-ORF3 and E4-ORF6 target the MRN DNA repair complex. In response to infection by Ad lacking the E4 region, the MRN complex associates with virus replication centers and activates a DNA damage response (DDR) (Carson et al., 2009; Karen et al., 2009; Stracker, Carson, and Weitzman, 2002). Ultimately, the DDR severely inhibits viral DNA replication and triggers the formation of viral genomic mutimers termed concatamers (Stracker, Carson, and Weitzman, 2002). Disruption of the MRN complex, through E4-ORF6-dependent degradation or recruitment into E4-ORF3-containing nuclear tracks is sufficient to rescue this replication defect (Evans and Hearing, 2005; Lakdawala et al., 2008; Mathew and Bridge, 2008). Like E4-ORF6, E4-ORF3 also targets p53. Acting upon p53 indirectly, E4-ORF3 down-regulates p53 target gene expression by promoting the formation of heterochromatin at p53 target promoter regions (Soria et al., 2010). E4-ORF3 also can impede the host cell, interferon-mediated antiviral response by sequestering PML, the nucleating factor in PML nuclear bodies (Ullman and Hearing, 2008; Ullman, Reich, and Hearing, 2007). Recently, we have shown that E4-ORF3 targets TIF1α, a protein implicated in several nuclear hormone receptor signaling pathways (Yondola and Hearing, 2007). Although the functional significance of this interaction remains unknown, the ability of E4-ORF3 to relocalize of TIF1α is conserved across multiple Ad serotypes (Yondola and Hearing, 2007).

TIF1α belongs to the transcriptional intermediary factor 1 (TIF1) family of proteins, consisting of four known members in humans--TIF1α, TIF1β, TIF1γ, and TIF1δ--as well as drosophila, murine, and zebrafish orthologs. Acting as coregulators of gene expression, TIF1 family proteins influence a wide array of gene expression pathways. Influencing the RA signaling pathway, TIF1α responds to RA by associating with nuclear receptors at the retinoic acid response element (RARE), where it regulates gene expression and ultimately promotes growth suppression (Khetchoumian et al., 2007; Zhong et al., 1999). Implicated as a tumor suppressor protein, loss of TIF1α leads to an increase in hepatic tumors in null mice (Khetchoumian et al., 2007). Furthermore, TIF1α has been shown to promote p53 ubiquitination, leading to its proteosome-dependent degradation (Allton et al., 2009). TIF1β acts as a corepressor of gene expression. Associating with promoter regions through interactions with DNA-bound KRAB domain containing proteins, TIF1β recruits chromatin modifiers such as HP1 family proteins to facilitate chromatin remodeling and transcriptional silencing (Ryan et al., 1999; Sripathy, Stevens, and Schultz, 2006). Acting in the TGFβ signaling pathway, TIF1γ plays a key role in ectoderm production in Xenopus (Dupont et al., 2009; Dupont et al., 2005), as well as erythroid production in humans (He et al., 2006). Recent evidence suggests a role for TIF1γ in promoting zebrafish erythroid development as part of a Pol II containing transcription complex (Bai et al., 2010; Ransom et al., 2004). Furthermore, the loss of TIF1γ has been implicated in the development of pancreatic cancer

(Vincent et al., 2009). TIF1δ acts as a testis-specific transcriptional corepressor that can interact with chromatin modifier HP1γ (Khetchoumian et al., 2004).

TIF1 family proteins fall into the greater tripartite motif (TRIM) protein family. Characterized by an N-terminal RBCC motif, TRIM family proteins contain three domains of conserved order and spacing: a **R**ING finger, one or two **B**-boxes, and a **C**oiled-**C**oil domain. Binding two zinc atoms in a cross brace motif, the RING finger domain is often associated with E3 ubiquitin ligase activity (Reviewed in (Meroni and Diez-Roux, 2005). Suggested to possess a similar quaternary structure as the RING domain (Tao et al., 2008), the B-box domain also coordinates zinc atoms. Two forms of this motif exist, B1 and B2, with differing patterns of histidine and cysteine residues critical for zinc coordination. TIF1 family proteins contain tandem B1 and B2 domains. The Coiled-Coil motif often mediates homomultimer formation and consists of a series of 1 to 3 amphipathic coiled subdomains (Peng et al., 2000; Peng, Feldman, and Rauscher, 2002; Reymond et al., 2001). TRIM family proteins contain the greatest sequence diversity in their C-terminal half, but often contain one or multiple C-terminal conserved protein folding motifs. TIF1 family proteins all contain C-terminal PHD/bromo domains.

We have previously demonstrated that E4-ORF3 targets TIF1α, but not the related TIF1β protein, for nuclear track localization in a manner dependent on the N-terminal RBCC motif (Yondola and Hearing, 2007). In this paper, we introduce TIF1γ as a novel E4-ORF3 track colocalizing protein and further characterize the ability of E4-ORF3 to target cellular proteins. We wished to determine which specific TIF1 protein sequences are sufficient for E4-ORF3-directed relocalization and how E4-ORF3 selectively targets TIF1α and TIF1γ without affecting TIF1β. Taking advantage of the homologous nature, yet differing recruitment capabilities of these proteins, we generated a series of EYFP-fusion constructs to map the ability of specific TIF1 subdomains to interact with E4-ORF3 under varying protein contexts. Using a series of isolated TIF1 protein segments, we demonstrate that E4-ORF3 associates with the Coiled-Coil domains of TIF1α, TIF1β, and TIF1γ. Furthermore, we generated a series of TIF1α/β and TIF1γ/β chimeric proteins whose localization patterns imply that the presence of the C-terminal portion of TIF1β interferes with this interaction. These results suggest that E4-ORF3 targets TIF1 family members through a loosely homologous sequence and that the accessibility of this sequence influences the ability of E4-ORF3 to recruit these proteins into nuclear tracks.

Results

E4-ORF3 relocalizes TIF1γ in vivo and binds TIF1γ in vitro

In order to examine if the E4-ORF3 protein alters the localization of endogenous TIF1γ *in vivo*, indirect immunofluorescence analyses were performed (Fig. 1). In uninfected HeLa cells, TIF1γ staining appeared generally uniform throughout the nucleus with some underlying foci (Fig. 1A). The TIF1γ-containing foci were found to colocalize with PML nuclear bodies (Figs. 1B, 1C; arrows). Six hours after infection with wild-type Ad5, the TIF1γ protein was relocalized into nuclear track structures (Fig. 1D) that colocalized with E4-ORF3 (Figs. 1E, 1F), although not all TIF1γ was reorganized at this early time point during infection. TIF1γ relocalization was more complete at early times after infection when a higher multiplicity of infection was used (Fig. 1G) indicating that the E4-ORF3 protein may be limiting. This reorganization of TIF1γ during Ad infection required the E4-ORF3 protein since no change in TIF1γ localization was evident in cells infected with an E4-ORF3 mutant virus (Fig. 1H; infected cells identified using an antibody against the Ad DNA binding protein, DBP, Figs 1I, 1J). At late times after infection with wild-type Ad5, TIF1γ reorganization into E4-ORF3-containing tracks was nearly complete (Figs. 1K–M). We next examined if the E4-ORF3 protein binds to TIF1γ *in vitro* using a coimmunoprecipitation

assay. HeLa cells were infected with Ad E1-replacement vectors that constitutively expresses HA-tagged wild-type E4-ORF3 or a nonfunctional mutant protein ($N_{82}A$; (Stracker, Carson, and Weitzman, 2002); Evans and Hearing, 2005). A rabbit polyclonal antibody directed against TIF1γ was used for immunoprecipitation and coprecipitation of wild-type or mutant E4-ORF3 was examined by Western blot using an anti-HA antibody (Fig. 2). Equal levels of wild-type and mutant E4-ORF3 proteins were evident in the starting cell extracts (lanes 1–3, bottom), but only the wild-type E4-ORF 3 protein coprecipitated with endogenous TIF1γ (lanes 4–6, bottom). Similar levels of TIF1γ were evident in the starting cell extracts and immunoprecipitates, although we note somewhat reduced TIF1γ levels in wild-type Ad5-infected samples (top panel). We conclude that the E4-ORF3 protein induces TIF1γ relocalization in Ad-infected cells *in vivo* and that wild type E4-ORF3, but not a nonfunctional mutant protein, binds TIF1γ *in vitro*.

E4-ORF3 targets the coiled-coil domain of TIF1α, TIF1β, and TIF1γ

Previously published results demonstrated that the RBCC domain of TIF1α is necessary and sufficient to mediate colocalization with E4-ORF3 (Yondola and Hearing, 2007). To map the amino acid sequences required for interaction with E4-ORF3 to within a specific TIF1α protein folding motif, we generated a series of recombinant EYFP-TIF1α fusion proteins (Fig. 3) consisting of the RING finger domain (EYFP-αR), the B-box domain (EYFP-αBB), or the Coiled-Coil domain (EYFP-αCC) fused to EYFP. Vectors that express these fusion proteins were transfected into HeLa cells on coverslips, which were then infected with wild-type Ad5 for eighteen hours, and then fixed and immunostained for the E4-ORF3 protein (Fig. 4). Expression of E4-ORF3 failed to lead to the relocalization of EYFP-αRING or EYFP-αB-Box (data not shown). When expressed in uninfected cells, EYFP-αCC displayed both nuclear and cytoplasmic expression patterns (Fig. 4A). Nuclear localizing EYFP-αCC was clearly brought into E4-ORF3-colocalizing tracks following Ad infection (Figs. 4B–D), suggesting that the coiled-coil domain of TIF1α is sufficient for E4-ORF3-induced relocalization.

As E4-ORF3 possesses the ability to target the Coiled-Coil domain of TIF1α, we hypothesized that E4-ORF3 would also target the Coiled-Coil domain of TIF1γ. Equivalent constructs consisting of the EYFP-tagged Coiled-Coil domains of TIF1β (EYFP-βCC) and TIF1γ (EYFP-γCC) were generated (Fig. 3). Vectors that express these fusion proteins were transfected into HeLa cells that were subsequently infected with wild-type Ad5. In uninfected cells, EYFP-βCC maintained a diffuse, nuclear staining pattern (Fig. 4E) whereas EYFP-γCC could be detected diffusely spread throughout the cell with prominent cytoplasmic staining (Fig. 4I). At high levels of expression, EYFP-γCC displayed a tendency to form aggregates, although this was not the case for EYFP-βCC. Interestingly, E4-ORF3 expression led to the rearrangement of the Coiled-Coil domains of both TIF1β and TIF1γ (Figs. 4F–H and 4J–L), although cytoplasmic EYFP-γCC could still be detected.

Although the Coiled-Coil domain of TIF1β colocalized with the E4-ORF3 protein in nuclear tracks, the corresponding full-length protein does not (Yondola and Hearing, 2007). As Coiled-Coil domains often mediate protein-protein interactions, one possibility is that isolation of this region of TIF1β permits track localization through an interaction with an endogenous Coiled-Coil-containing track-associated protein. To elucidate the potential for promiscuous track localization, we generated an EYFP-tagged Coiled-Coil construct from PML (EYFP-PMLCC; Fig. 3), a protein brought into E4-ORF3-containing tracks through a region mapped outside of the Coiled-Coil motif (Leppard et al., 2009). To minimize protein aggregation, we expressed this construct in HeLa cells that were subsequently infected with wild-type Ad5 for eight hours. The EYFP-PML-CC fusion protein remained diffusely localized throughout infected cells (Figs. 4N–P), displaying a similar localization pattern as that seen in uninfected cells (Fig. 4M). At higher levels of expression, EYFP-PML-CC

displayed a tendency to form multiple nuclear and cytoplasmic punctate aggregates. In some instances, E4-ORF3 could be seen colocalizing with EYFP-PML-CC in these punctate aggregates (data not shown). However, the high level of expression required, altered appearance, and presence in the cytoplasm differed greatly from the typical E4-ORF3 track localization. As this atypical E4-ORF3 localization pattern was only seen during instances of high levels of EYFP-PML-CC expression, it is likely due to protein over-expression and possible protein aggregation, rather than resulting from a direct E4-ORF3/EYFP-PML-CC interaction. Together, these data support the idea that the E4-ORF3 protein specifically interacts with the Coiled-Coil domains of TIF1 proteins.

Protein context influences the ability of E4-ORF3 to interact with TIF1 Coiled-Coil domains

One explanation for these results suggests that the E4-ORF3 protein may target a sequence found in all three TIF1 Coiled-Coil motifs and that its isolation removes an interfering factor found within full-length TIF1β. In order to examine the ability of the TIF1 Coiled-Coil domains to interact with E4-ORF3 in the context of full-length TIF1 proteins, we generated a series of EYFP-tagged protein chimeras consisting of TIF1β containing the Coiled-Coil domain of TIF1α or TIF1γ (EYFP-TIF1β-αCC, EYFP-TIF1β-γCC; Fig. 3) and TIF1α containing the Coiled-Coil domain of TIF1β (EYFP-TIF1α-βCC; Fig. 3). All three fusion proteins displayed a diffuse, nuclear staining pattern in uninfected cells (Figs. 5A, 5E, and 5I). Following infection with wild-type Ad5, E4-ORF3 rearranged EYFP-TIF1α-βCC into E4-ORF3-colocalizing nuclear tracks (Figs. 5B–D). EYFP-TIF1β-αCC and EYFP-TIF1β-γCC retained a diffuse nuclear localization pattern in cells infected with wild-type Ad5 (Figs. 5F–H and 5J–L). The ability of all three Coiled-Coil motifs to direct the localization in the context of TIF1α or TIF1γ, but not TIF1β, suggests that additional sequences present in full-length TIF1β inhibits an intrinsic association ability with the E4-ORF3 protein.

The C-terminal half of TIF1β interferes with the ability of E4-ORF3 to target the TIF1β Coiled-Coil domain

If a portion of TIF1β interferes with the ability of E4-ORF3 to interact with the Coiled-Coil domain, its removal should facilitate E4-ORF3-induced track localization. As TIF1α, TIF1β, and TIF1γ share a homologous N-terminal RBCC domain, we wished to determine if the removal of the C-terminal half (CTH) of TIF1β, consisting of the divergent middle region and a conserved PHD/Bromo domain, permitted E4-ORF3-mediated relocalization. The RBCC domain of TIF1β was fused to EYFP (EYFP-βRBCC; Fig. 3) and the expression vector was transfected into HeLa cells. In uninfected cells, EYFP-TIF1β displayed a diffuse, nuclear staining pattern whereas EYFP-βRBCC was seen diffusely spread throughout the cell (Figs. 6A and 6E). Eighteen hours after infection with wild-type Ad5, EYFP-TIF1β retained a diffuse nuclear staining pattern, however, EYFP-βRBCC associated with E4-ORF3 in nuclear tracks (Figs. 6B–D and 6F–H). To further demonstrate the ability of the CTH of TIF1β to interfere with E4-ORF3-induced relocalization, we generated an EYFP fusion protein consisting of the RBCC domain of TIF1α fused to the CTH of TIF1β (EYFP-TIF1α-βCTH; Fig. 3). We previously demonstrated that the EYFP-αRBCC was relocalized into nuclear tracks following E4-ORF3 expression (Yondola and Hearing, 2007). In contrast, EYFP-TIF1α-βCTH failed to colocalize with E4-ORF3 maintaining a diffuse, nuclear staining pattern similar to that seen in uninfected cells (Figs. 6I–L). This result indicates that the presence of the CTH of TIF1β interferes with the ability of E4-ORF3 to target the Coiled-Coil domain of TIF1α. Together, these results suggest that the CTH of TIF1β interferes with the ability of E4-ORF3 to access the Coiled-Coil motif of TIF1β.

We verified these results using a coimmunoprecipitation assay. Different EYFP-TIF1 fusion proteins were expressed in transfected HeLa cells and cells were then mock-infected or infected with a recombinant Ad vector that expresses wild-type, HA-tagged E4-ORF3

protein. EYFP-TIF1 proteins were immunoprecipitated from cell extracts using an anti-GFP antibody that recognizes EYFP. Binding of HA-E4-ORF3 was assessed by Western blot analysis using an anti-HA antibody (Fig 7). While the levels of the EYFP-TIF1 fusion proteins immunoprecipitated varied between constructs, EYFP-TIF1α and EYFP-TIF1γ, but not EYFP-TIF1β, coprecipitated with HA-E4-ORF3. In agreement with the immunofluorescence results, EYFP-TIF1α-βCC bound HA-E4-ORF3, whereas neither EYFP-TIF1β-αCC nor EYFP-TIF1β-γCC did despite high levels of immunoprecipitated proteins in these samples. In further support, the EYFP-TIF1α-βCTH fusion protein did not detectably coprecipitate with HA-E4-ORF3. These results verify the immunofluorescence assays and confirm that E4-ORF3-induced TIF1 relocalization into nuclear tracks requires specific interactions between these cellular and viral proteins.

Discussion

In this study, we demonstrate that the Ad5 E4-ORF3 protein binds to endogenous TIF1γ *in vitro* and relocalizes endogenous TIF1γ into E4-ORF3-containing tracks *in vivo*. Further, we show that the Coiled-Coil domain is the only isolated TIF1α segment brought into nuclear tracks; the RING, B box, and C-terminal half of TIF1α--consisting of the middle region, PHD, and Bromo domain--fail to colocalize with E4-ORF3 when expressed individually as EYFP fusion proteins (this study, and (Yondola and Hearing, 2007)). In addition, E4-ORF3 holds the ability to rearrange the isolated Coiled-Coil domains of TIF1β and TIF1γ. However, Coiled-Coil domains expressed in the context of full-length TIF1β (EYFP-TIF1β-αCC and EYFP-TIF1β-γCC) as well as TIF1β, fail to colocalize with E4-ORF3 in nuclear tracks. These data suggest that the E4-ORF3 protein does not simply target a consensus sequence found in TIF1α and TIF1γ but absent from TIF1β. The ability of TIF1 Coiled-Coil domains to permit track localization in isolation or in the context of TIF1α, but not in the context of TIF1β, suggests that a TIF1β-specific feature interferes with the ability of E4-ORF3 to interact with this TIF1 protein. We acknowledge that tagging the different proteins with EYFP at their N-termini may influence their behavior, but collectively all of the data are consistent with the conclusion that E4-ORF3 targets the Coiled-Coil domains of TIF1 proteins for relocalization.

As Coiled-Coil domains often mediate protein-protein interactions, it is possible that these EYFP-TIF1 fusion proteins might gain the ability to interact with a track-localizing protein that contains a Coiled-oil motif, such as PML or endogenous TIF1α, and are relocalized by E4-ORF3 in an indirect manner. However, the absence of relocalization of EYFP-PML-CC following E4-ORF3 expression detracts from this hypothesis. Our results indicate that the Coiled-Coil domains from all three tested TIF1 family proteins contain a sequence that is a target for E4-ORF3-induced relocalization. Since the addition of the βCTH to the RBCC domain of TIF1α disrupts track localization, our results suggest that the βCTH actively interferes with E4-ORF3 relocalization of the full-length TIF1β protein. The nature of this interference, however, remains unknown. In addition to a conserved PHD/bromo domain, the βCTH contains the middle region--a segment of low sequence conservation between TIF1α, TIF1β, and TIF1γ (Venturini et al., 1999). It is possible that a sequence unique to TIF1β generates a protein folding conformation that physically blocks the ability of E4-ORF3 to associate with the TIF1β Coiled-Coil domain. A recent publication characterizes potential synergistic activities between TIF1α, TIF1β, and TIF1γ in the context of murine hepatocellular carcinoma development and demonstrates the presence of a TIF1α- and TIF1γ-containing protein complex as well as a less abundant TIF1α-, TIF1β-, and TIF1γ-containing complex (Herquel et al., 2011). It is interesting to speculate that the same properties that facilitate the formation of these complexes play a role in permitting or disallowing E4-ORF3-mediated track localization.

Recent work suggests that E4-ORF3 relocalizes PML through a direct interaction with a short amino acid sequence unique to PML isoform II-specific exon 7b (Hoppe et al., 2006; Leppard et al., 2009). An alignment of this region, spanning PMLII amino acids 645–684, with other known E4-ORF3-associated proteins including TIF1α, revealed a short, loosely homologous sequence motif. In agreement with our data, this short sequence can be found within the Coiled-Coil domains of TIF1α (residues 375–391), TIF1β (residues 361–377), and TIF1γ (residues 427–443). Interestingly, the E4-ORF3-interacting region in PMLII exon 7b falls outside the PML N-terminal RBCC motif, indicating that the Coiled-Coil domain of PML is neither necessary nor sufficient for E4-ORF3-induced relocalization. Furthermore, the ability of E4-ORF3 to target the Coiled-Coil domain of TIF1β outside of the context of the wild-type protein suggests that protein context, in addition to the presence of a specific target sequence, plays a role in E4-ORF3-mediated protein relocalizaiton.

Whereas much is known about the roles TIF1α and TIF1γ play under normal cellular conditions, the functional significance of their relocalization during Ad infection remains unclear. The rearrangement of other known E4-ORF3 targets (e.g., PML and MRN), serves to inhibit their anti-viral activities. Rearrangement by E4-ORF3 could function as a mechanism to target a cellular process dependent on these two proteins. Acting as transcriptional coregulators, TIF1α influences the retinoic acid signaling pathway while TIF1γ affects TGFβ-dependent signaling as well as transcriptional elongation (Bai et al., 2010; Dupont et al., 2009; He et al., 2006; Khetchoumian et al., 2007). It is possible that E4-ORF3 sequesters TIF1α and TIF1γ to alter their downstream transcriptional target levels. TIF1α and TIF1γ also have both been shown to contain E3 ubiquitin ligase activities in certain contexts (Allton et al., 2009; Dupont et al., 2009; Dupont et al., 2005). Recruitment into nuclear tracks could serve to regulate ubiquitin ligase activity, either by preventing TIF1α and TIF1γ from promoting the ubiquitination of target proteins or by promoting the ubiquitination of one or more track-associated proteins. The E4-ORF3 protein previously was shown to facilitate MRN protein degradation in Ad-infected cells (Liu, Shevchenko, and Berk, 2005). Finally, E4-ORF3-dependent rearrangement of TIF1 proteins could provide an additional way for Ad to influence cell proliferation. Whereas Ad targets terminally differentially epithelial cells for infection, it has evolved multiple mechanisms to force the cell to return to S-phase, generating a cellular environment more conducive to productive virus replication (reviewed in (Berk, 2005)). Over-expression of either TIF1α or TIF1γ has been shown to retard cell growth and these proteins have been linked as tumor suppressors in murine and human cancer (Khetchoumian et al., 2007; Vincent et al., 2009). E4-ORF3 may influence cellular growth by inhibiting the roles of these TIF1 proteins as negative regulators of cellular proliferation.

The E4-ORF3-dependent reorganization of TIF1α and TIF1γ is an attractive target for future studies as many TRIM family proteins possess functions that participate in the cellular innate immune response; as many as 27 display altered expression patterns in the presence of interferon (Carthagena et al., 2009). Several TRIM proteins have been implicated as effectors in the IRF3/IRF7- and NF-κB-dependent signaling pathways, modifying interferon and proinflammatory cytokine production, respectively (Ozato et al., 2008). For example, TRIM25 induces ubiquitination of cytosolic RNA sensor RIG-I, which ultimately promotes downstream IFN-β expression (Gack et al., 2007). Also known as RFP, TRIM27 binds to protein kinases TBK1, IKKα, IKKβ, and IKKε which promotes the inhibition of IRF3- and NF-κB-dependent signaling (Zha et al., 2006). PML, TRIM19, is implicated in the restriction of multiple DNA and RNA virus replication cycles (reviewed in (Everett and Chelbi-Alix, 2007)). Other TRIM family proteins function to restrict virus propagation directly. TRIM22 expression is correlated with a decrease in HIV-1 long terminal repeat driven gene expression (Kajaste-Rudnitski et al., 2011) and has been shown to inhibit HIV particle production by interfering with the localization of structural protein gag and virus

particle release (Barr, Smiley, and Bushman, 2008). Implicated as a factor that can restrict HIV infection, rhesus monkey TRIM5α (TRIM5α_{rh}) has been shown to promote premature capsid uncoating as well as facilitate gag protein degradation (Sakuma et al., 2007; Stremlau et al., 2006). TIF1α and TIF1γ may possess similar anti-viral activities, but additional studies are needed to address this possibility.

Materials and methods

Plasmid construction

EYFP fusion proteins were generated using pEYFP-C1 (Clontech). Primer pairs used for fusion protein cloning are shown in Table 1. TIF1α and TIF1β cDNA clones were purchased from OriGene Technologies (Rockville, MD). A TIF1γ cDNA clone was provided by Dr. Joan Massagué (Memorial Sloan Kettering Cancer Center, New York, NY). EYFP-αRING (primer set 1), EYFP-αBbox, (primer set 2), EYFP-αCC (primer set 3), EYFP-βCC (primer set 4), EYFP-γCC (primer set 5), EYFP-PML-CC (primer set 11), and EYFP-βRBCC (primer set 12) were generated using polymerase chain reaction (PCR)-directed amplification of TIF1- or PML-specific protein coding sequences. Amplicons were cut with BglII and XmaI restriction endonucleases and incorporated into pEYFP-C1 cut with the same enzymes. EYFP-βRBCC was cut with BglII and BamHI before incorporation into pEYFP-C1. EYFP-TIF1β-αRB was generated through the PCR-directed amplification of the coiled-coil and CTH of TIF1β (primer set 8), digestion with HindIII and BglII, and ligation into an EYFP-TIF1α vector digested with BamHI and HindIII. EYFP-TIF1β-αRBCC was generated through the PCR directed amplification of αRBCC (primer set 7a) and βCTH (primer set 7b), ligation via PCR, and insertion into the pEYFP-C1 vector. EYFP-TIF1α-βCC was generated through the PCR-directed amplification of αCTH (primer set 6), digestion with BglII and XbaI, and insertion into EYFP-TIF1β-αRB cleaved with BamHI and XbaI. EYFP-TIF1β-αCC was generated through the PCR-directed amplification of βRB (primer set 9), cleavage with BglII and HindIII, and insertion into EYFP-TIF1β-αRBCC digested with BglII and HindIII. EYFP-TIF1β-γCC was generated through the PCR-directed amplification of γCC (primer set 10). The PCR amplicon and EYFP-TIF1β-αCC vector were then digested with HindIII and BamHI and ligated together.

Cell culture, transfection, and virus infections

Experiments were carried out in HeLa cells (ATCC) grown in Dulbecco's modified eagle medium supplemented with 10% bovine calf serum, unless otherwise specified. Cells were transfected using Fugene 6 (Roche) or polyethylenimine (PEI) (Polysciences Inc.) via the manufacturer's instruction, proteins were allowed to express overnight, and cells were subsequently infected with virus, when indicated. Cells were infected with wild-type Ad5 at 200 virus particles/cell or with Ad E1-replacement viruses that express HA-tagged wild-type or mutant E4-ORF3 at 500 virus particles/cell for 1 hour before the addition of new media. The following viruses were used: phenotypically wild-type Ad5 *dl*309 (Jones and Shenk, 1979)), and Ad-CMV-HA-ORF3-WT or –HA-ORF3-N82A (E1A replacement viruses that expresses E4-ORF3 fused to an HA epitope under the control of a CMV promoter (Evans and Hearing, 2003; Evans and Hearing, 2005).

Immunofluoresence analysis

Cells were grown on glass coverslips, transfected, and then infected using the conditions described above. Between 16 and 18 hours post-infection, cells were washed with PBS, fixed using −20°C methanol, and blocked for 1 hour at room temperature with 10% goat serum diluted into PBS. Primary antibody consisting of either rat monoclonal anti-E4-ORF3 (mAb 6A11 (Nevels et al., 1999)), rabbit polyclonal anti-TIF1γ (generated at Lampire Biological Laboratories, Pipersville, PA), or anti-PML (PG-M3, Santa Cruz Biotechnology)

diluted into 10% goat serum block was applied to coverslips for 1 hour at room temperature. Coverslips were then washed with PBS and incubated with secondary antibody consisting of tetramethyl rhodamine isothiocyanate (TRITC) labeled anti-rat (Invitrogen), or fluorescein isothiocyanate (FITC) labeled anti-rabbit (Invitrogen) for thirty minutes at room temperature in the dark. Coverslips were mounted on slides using ImmunoMount (Thermo Shandon). The microscope used was a Zeiss Axiovert 200M Digital Deconvolution Microscope fitted with a Chroma filter set and an apotome and images were captured with a Peltier-cooled CCD Axiocam HRm camera and analyzed with Axiovision 4.5 software.

Immunoprecipitation and western blot analysis

Ten cm dishes of HeLa cells were transfected with 5μg of each EYFP expression vector indicated and infected with Ad-CMV-HA-ORF3-WT, as described above. At 18 hours post-infection, cells were washed with PBS, collected, and resuspended in F-lysis buffer (50 mM Tris pH 7.4, 50 mM NaCl, 10% glycerol, 0.5% Triton X-100) supplemented with protease inhibitors (phenylmethylsulfonyl fluoride, benzamidine, pepstatin, leupeptin, and aprotinin). The cellular lysate was incubateded on ice for twenty minutes, sonicated at 50% duty, setting 5, for 20 pulses on ice, and then centrifuged for 15 minutes, 16000 × g, at 4°C. Protein A beads were used to preclear the soluble lysate during a 1 hour rotation at 4°C. The samples were cleared by centrifugation, the lysate was incubated with rabbit anti-GFP (Lifespan Biosciences) and protein A beads with rotation overnight at 4°C. The immunoprecipitates were then washed five times with F-lysis buffer containg protease inhibitors and resuspended in 40 μl 2× Laemmli sample buffer (1.2% SDS, 150 mM Tris pH 6.8, 50 mM dithiothreitol). Samples were incubated at 95°C for 5 minutes and subjected to SDS-PAGE. An 18.5% gel was used to resolve HA-ORF3 whereas a 7.5% gel was used to resolve the EYFP-tagged fusion proteins. Proteins were transferred to polyvinylidene fluoride (PVDF) (Hybond-P, GE Healthcare) membranes overnight at 40mA. PVDF membranes were blocked for 1 hour with 3% BSA in PBS, then incubated with primary antibody, consisting of either mouse monoclonal anti-HA (Abcam) or anti-GFP rabbit polyclonal antibody (Lifespan Biosciences), overnight at 4°C.. The membranes were washed and anti-mouse HRP and anti-rabbit HRP (GE Healthcare) secondary antibodies were applied to membranes for thirty minutes. Immobilon chemiluminescent HRP substrate (Millipore) was used for detection.

Acknowledgments

We thank Drs. Joan Massagué and Wei He (Memorail Sloan Kettering Cancer Center, New York, NY) for a rabbit anti-TIF1γ antibody used during early stages of these studies and for a TIF1γ cDNA clone. We acknowledge the excellent technical assistance of Ilana Shoshani. We thank members of our laboratory for informed discussions. This work was supported by NIH grant CA122677. E.V. and M.Y. were supported by NIH Training Grant CA009176.

References

Allton K, Jain AK, Herz HM, Tsai WW, Jung SY, Qin J, Bergmann A, Johnson RL, Barton MC. Trim24 targets endogenous p53 for degradation. Proc Natl Acad Sci U S A. 2009; 106(28):11612–6. [PubMed: 19556538]

Bai X, Kim J, Yang Z, Jurynec MJ, Akie TE, Lee J, LeBlanc J, Sessa A, Jiang H, DiBiase A, Zhou Y, Grunwald DJ, Lin S, Cantor AB, Orkin SH, Zon LI. TIF1gamma controls erythroid cell fate by regulating transcription elongation. Cell. 2010; 142(1):133–43. [PubMed: 20603019]

Baker A, Rohleder KJ, Hanakahi LA, Ketner G. Adenovirus E4 34k and E1b 55k oncoproteins target host DNA ligase IV for proteasomal degradation. J Virol. 2007; 81(13):7034–40. [PubMed: 17459921]

Barr SD, Smiley JR, Bushman FD. The interferon response inhibits HIV particle production by induction of TRIM22. PLoS Pathog. 2008; 4(2):e1000007. [PubMed: 18389079]

Berk AJ. Recent lessons in gene expression, cell cycle control, and cell biology from adenovirus. Oncogene. 2005; 24(52):7673–85. [PubMed: 16299528]

Blanchette P, Kindsmuller K, Groitl P, Dallaire F, Speiseder T, Branton PE, Dobner T. Control of mRNA export by adenovirus E4orf6 and E1B55K proteins during productive infection requires E4orf6 ubiquitin ligase activity. J Virol. 2008; 82(6):2642–51. [PubMed: 18184699]

Bridge E, Ketner G. Redundant control of adenovirus late gene expression by early region 4. J Virol. 1989; 63(2):631–8. [PubMed: 2911117]

Carson CT, Orazio NI, Lee DV, Suh J, Bekker-Jensen S, Araujo FD, Lakdawala SS, Lilley CE, Bartek J, Lukas J, Weitzman MD. Mislocalization of the MRN complex prevents ATR signaling during adenovirus infection. EMBO J. 2009; 28(6):652–62. [PubMed: 19197236]

Carthagena L, Bergamaschi A, Luna JM, David A, Uchil PD, Margottin-Goguet F, Mothes W, Hazan U, Transy C, Pancino G, Nisole S. Human TRIM gene expression in response to interferons. PLoS ONE. 2009; 4(3):e4894. [PubMed: 19290053]

Dallaire F, Blanchette P, Groitl P, Dobner T, Branton PE. Identification of integrin alpha3 as a new substrate of the adenovirus E4orf6/E1B 55-kilodalton E3 ubiquitin ligase complex. J Virol. 2009; 83(11):5329–38. [PubMed: 19297475]

Dobner T, Horikoshi N, Rubenwolf S, Shenk T. Blockage by adenovirus E4orf6 of transcriptional activation by the p53 tumor suppressor. Science. 1996; 272(5267):1470–3. [PubMed: 8633237]

Dupont S, Mamidi A, Cordenonsi M, Montagner M, Zacchigna L, Adorno M, Martello G, Stinchfield MJ, Soligo S, Morsut L, Inui M, Moro S, Modena N, Argenton F, Newfeld SJ, Piccolo S. FAM/USP9x, a deubiquitinating enzyme essential for TGFbeta signaling, controls Smad4 monoubiquitination. Cell. 2009; 136(1):123–35. [PubMed: 19135894]

Dupont S, Zacchigna L, Cordenonsi M, Soligo S, Adorno M, Rugge M, Piccolo S. Germ-layer specification and control of cell growth by Ectodermin, a Smad4 ubiquitin ligase. Cell. 2005; 121(1):87–99. [PubMed: 15820681]

Evans JD, Hearing P. Distinct roles of the Adenovirus E4 ORF3 protein in viral DNA replication and inhibition of genome concatenation. J Virol. 2003; 77(9):5295–304. [PubMed: 12692231]

Evans JD, Hearing P. Relocalization of the Mre11-Rad50-Nbs1 complex by the adenovirus E4 ORF3 protein is required for viral replication. J Virol. 2005; 79(10):6207–15. [PubMed: 15858005]

Everett RD, Chelbi-Alix MK. PML and PML nuclear bodies: implications in antiviral defence. Biochimie. 2007; 89(6–7):819–30. [PubMed: 17343971]

Gack MU, Shin YC, Joo CH, Urano T, Liang C, Sun L, Takeuchi O, Akira S, Chen Z, Inoue S, Jung JU. TRIM25 RING-finger E3 ubiquitin ligase is essential for RIG-I-mediated antiviral activity. Nature. 2007; 446(7138):916–920. [PubMed: 17392790]

Halbert DN, Cutt JR, Shenk T. Adenovirus early region 4 encodes functions required for efficient DNA replication, late gene expression, and host cell shutoff. J Virol. 1985; 56(1):250–7. [PubMed: 4032537]

Harada JN, Shevchenko A, Pallas DC, Berk AJ. Analysis of the adenovirus E1B-55K-anchored proteome reveals its link to ubiquitination machinery. J Virol. 2002; 76(18):9194–206. [PubMed: 12186903]

He W, Dorn DC, Erdjument-Bromage H, Tempst P, Moore MA, Massague J. Hematopoiesis controlled by distinct TIF1gamma and Smad4 branches of the TGFbeta pathway. Cell. 2006; 125(5):929–41. [PubMed: 16751102]

Herquel B, Ouararhni K, Khetchoumian K, Ignat M, Teletin M, Mark M, Bechade G, Van Dorsselaer A, Sanglier-Cianferani S, Hamiche A, Cammas F, Davidson I, Losson R. Transcription cofactors TRIM24, TRIM28, and TRIM33 associate to form regulatory complexes that suppress murine hepatocellular carcinoma. Proc Natl Acad Sci U S A. 2011

Hoppe A, Beech SJ, Dimmock J, Leppard KN. Interaction of the adenovirus type 5 E4 Orf3 protein with promyelocytic leukemia protein isoform II is required for ND10 disruption. J Virol. 2006; 80(6):3042–9. [PubMed: 16501113]

Huang MM, Hearing P. Adenovirus early region 4 encodes two gene products with redundant effects in lytic infection. J Virol. 1989; 63(6):2605–15. [PubMed: 2724411]

Jones N, Shenk T. Isolation of adenovirus type 5 host range deletion mutants defective for transformation of rat embryo cells. Cell. 1979; 17(3):683–9. [PubMed: 476833]

Kajaste-Rudnitski A, Marelli SS, Pultrone C, Pertel T, Uchil PD, Mechti N, Mothes W, Poli G, Luban J, Vicenzi E. TRIM22 Inhibits HIV-1 Transcription Independently of Its E3 Ubiquitin Ligase Activity, Tat, and NF-{kappa}B-Responsive Long Terminal Repeat Elements. J Virol. 2011; 85(10):5183–96. [PubMed: 21345949]

Karen KA, Hoey PJ, Young CS, Hearing P. Temporal regulation of the Mre11-Rad50-Nbs1 complex during adenovirus infection. J Virol. 2009; 83(9):4565–73. [PubMed: 19244322]

Khetchoumian K, Teletin M, Mark M, Lerouge T, Cervino M, Oulad-Abdelghani M, Chambon P, Losson R. TIF1delta, a novel HP1-interacting member of the transcriptional intermediary factor 1 (TIF1) family expressed by elongating spermatids. J Biol Chem. 2004; 279(46):48329–41. [PubMed: 15322135]

Khetchoumian K, Teletin M, Tisserand J, Mark M, Herquel B, Ignat M, Zucman-Rossi J, Cammas F, Lerouge T, Thibault C, Metzger D, Chambon P, Losson R. Loss of Trim24 (Tif1alpha) gene function confers oncogenic activity to retinoic acid receptor alpha. Nat Genet. 2007; 39(12):1500–6. [PubMed: 18026104]

Lakdawala SS, Schwartz RA, Ferenchak K, Carson CT, McSharry BP, Wilkinson GW, Weitzman MD. Differential requirements of the C terminus of Nbs1 in suppressing adenovirus DNA replication and promoting concatemer formation. J Virol. 2008; 82(17):8362–72. [PubMed: 18562516]

Leppard KN, Emmott E, Cortese MS, Rich T. Adenovirus type 5 E4 Orf3 protein targets promyelocytic leukaemia (PML) protein nuclear domains for disruption via a sequence in PML isoform II that is predicted as a protein interaction site by bioinformatic analysis. J Gen Virol. 2009; 90(Pt 1):95–104. [PubMed: 19088278]

Liu Y, Shevchenko A, Berk AJ. Adenovirus exploits the cellular aggresome response to accelerate inactivation of the MRN complex. J Virol. 2005; 79(22):14004–16. [PubMed: 16254336]

Mathew SS, Bridge E. Nbs1-dependent binding of Mre11 to adenovirus E4 mutant viral DNA is important for inhibiting DNA replication. Virology. 2008; 374(1):11–22. [PubMed: 18234271]

Meroni G, Diez-Roux G. TRIM/RBCC, a novel class of 'single protein RING finger' E3 ubiquitin ligases. Bioessays. 2005; 27(11):1147–57. [PubMed: 16237670]

Nevels M, Tauber B, Kremmer E, Spruss T, Wolf H, Dobner T. Transforming potential of the adenovirus type 5 E4orf3 protein. J Virol. 1999; 73(2):1591–600. [PubMed: 9882365]

Orazio NI, Naeger CM, Karlseder J, Weitzman MD. The adenovirus E1b55K/E4orf6 complex induces degradation of the Bloom helicase during infection. J Virol. 2010

Ozato K, Shin DM, Chang TH, Morse HC 3rd. TRIM family proteins and their emerging roles in innate immunity. Nat Rev Immunol. 2008; 8(11):849–60. [PubMed: 18836477]

Peng H, Begg GE, Schultz DC, Friedman JR, Jensen DE, Speicher DW, Rauscher FJ 3rd. Reconstitution of the KRAB-KAP-1 repressor complex: a model system for defining the molecular anatomy of RING-B box-coiled-coil domain-mediated protein-protein interactions. J Mol Biol. 2000; 295(5):1139–62. [PubMed: 10653693]

Peng H, Feldman I, Rauscher FJ 3rd. Hetero-oligomerization among the TIF family of RBCC/TRIM domain-containing nuclear cofactors: a potential mechanism for regulating the switch between coactivation and corepression. J Mol Biol. 2002; 320(3):629–44. [PubMed: 12096914]

Querido E, Blanchette P, Yan Q, Kamura T, Morrison M, Boivin D, Kaelin WG, Conaway RC, Conaway JW, Branton PE. Degradation of p53 by adenovirus E4orf6 and E1B55K proteins occurs via a novel mechanism involving a Cullin-containing complex. Genes Dev. 2001; 15(23):3104–17. [PubMed: 11731475]

Ransom DG, Bahary N, Niss K, Traver D, Burns C, Trede NS, Paffett-Lugassy N, Saganic WJ, Lim CA, Hersey C, Zhou Y, Barut BA, Lin S, Kingsley PD, Palis J, Orkin SH, Zon LI. The zebrafish moonshine gene encodes transcriptional intermediary factor 1gamma, an essential regulator of hematopoiesis. PLoS Biol. 2004; 2(8):E237. [PubMed: 15314655]

Reymond A, Meroni G, Fantozzi A, Merla G, Cairo S, Luzi L, Riganelli D, Zanaria E, Messali S, Cainarca S, Guffanti A, Minucci S, Pelicci PG, Ballabio A. The tripartite motif family identifies cell compartments. EMBO J. 2001; 20(9):2140–51. [PubMed: 11331580]

Ryan RF, Schultz DC, Ayyanathan K, Singh PB, Friedman JR, Fredericks WJ, Rauscher FJ 3rd. KAP-1 corepressor protein interacts and colocalizes with heterochromatic and euchromatic HP1

proteins: a potential role for Kruppel-associated box-zinc finger proteins in heterochromatin-mediated gene silencing. Mol Cell Biol. 1999; 19(6):4366–78. [PubMed: 10330177]

Sakuma R, Noser JA, Ohmine S, Ikeda Y. Rhesus monkey TRIM5alpha restricts HIV-1 production through rapid degradation of viral Gag polyproteins. Nat Med. 2007; 13(5):631–5. [PubMed: 17435772]

Soria C, Estermann FE, Espantman KC, O'Shea CC. Heterochromatin silencing of p53 target genes by a small viral protein. Nature. 2010; 466(7310):1076–81. [PubMed: 20740008]

Sripathy SP, Stevens J, Schultz DC. The KAP1 corepressor functions to coordinate the assembly of de novo HP1-demarcated microenvironments of heterochromatin required for KRAB zinc finger protein-mediated transcriptional repression. Mol Cell Biol. 2006; 26(22):8623–38. [PubMed: 16954381]

Stracker TH, Carson CT, Weitzman MD. Adenovirus oncoproteins inactivate the Mre11-Rad50-NBS1 DNA repair complex. Nature. 2002; 418(6895):348–52. [PubMed: 12124628]

Stremlau M, Perron M, Lee M, Li Y, Song B, Javanbakht H, Diaz-Griffero F, Anderson DJ, Sundquist WI, Sodroski J. Specific recognition and accelerated uncoating of retroviral capsids by the TRIM5alpha restriction factor. Proc Natl Acad Sci U S A. 2006; 103(14):5514–9. [PubMed: 16540544]

Tao H, Simmons BN, Singireddy S, Jakkidi M, Short KM, Cox TC, Massiah MA. Structure of the MID1 tandem B-boxes reveals an interaction reminiscent of intermolecular ring heterodimers. Biochemistry. 2008; 47(8):2450–7. [PubMed: 18220417]

Ullman AJ, Hearing P. Cellular proteins PML and Daxx mediate an innate antiviral defense antagonized by the adenovirus E4 ORF3 protein. J Virol. 2008; 82(15):7325–35. [PubMed: 18480450]

Ullman AJ, Reich NC, Hearing P. Adenovirus E4 ORF3 protein inhibits the interferon-mediated antiviral response. J Virol. 2007; 81(9):4744–52. [PubMed: 17301128]

Venturini L, You J, Stadler M, Galien R, Lallemand V, Koken MH, Mattei MG, Ganser A, Chambon P, Losson R, de The H. TIF1gamma, a novel member of the transcriptional intermediary factor 1 family. Oncogene. 1999; 18(5):1209–17. [PubMed: 10022127]

Vincent DF, Yan KP, Treilleux I, Gay F, Arfi V, Kaniewski B, Marie JC, Lepinasse F, Martel S, Goddard-Leon S, Iovanna JL, Dubus P, Garcia S, Puisieux A, Rimokh R, Bardeesy N, Scoazec JY, Losson R, Bartholin L. Inactivation of TIF1gamma cooperates with Kras to induce cystic tumors of the pancreas. PLoS Genet. 2009; 5(7):e1000575. [PubMed: 19629168]

Weinberg DH, Ketner G. Adenoviral early region 4 is required for efficient viral DNA replication and for late gene expression. J Virol. 1986; 57(3):833–8. [PubMed: 3485200]

Woo JL, Berk AJ. Adenovirus ubiquitin-protein ligase stimulates viral late mRNA nuclear export. J Virol. 2007; 81(2):575–87. [PubMed: 17079297]

Yondola MA, Hearing P. The adenovirus E4 ORF3 protein binds and reorganizes the TRIM family member transcriptional intermediary factor 1 alpha. J Virol. 2007; 81(8):4264–71. [PubMed: 17287283]

Zha J, Han KJ, Xu LG, He W, Zhou Q, Chen D, Zhai Z, Shu HB. The Ret finger protein inhibits signaling mediated by the noncanonical and canonical IkappaB kinase family members. J Immunol. 2006; 176(2):1072–80. [PubMed: 16393995]

Zhong S, Delva L, Rachez C, Cenciarelli C, Gandini D, Zhang H, Kalantry S, Freedman LP, Pandolfi PP. A RA-dependent, tumour-growth suppressive transcription complex is the target of the PML-RARalpha and T18 oncoproteins. Nat Genet. 1999; 23(3):287–95. [PubMed: 10610177]

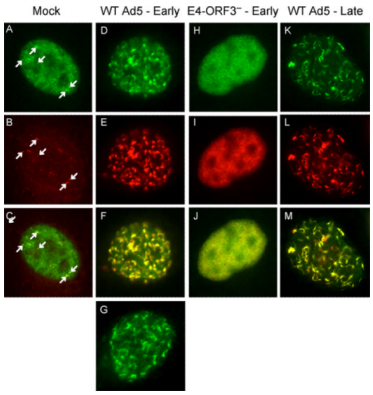

Fig. 1.

E4-ORF3 alters the localization of endogenous TIF1γ *in vivo*. **A.** Endogenous TIF1γ localization in mock-infected Hela cells was analyzed by indirect immunofluorescence using anti-TIF1γ primary antibody and FITC-conjugated secondary antibody. **B.** PML localization in the same cell using anti-PML primary antibody and TRITC-conjugated secondary antibody. **C.** Merge of panels **A** and **B**; arrows indicate colocalization of TIF1γ and PML nuclear bodies. **D–F.** TIF1γ localization at early times after infection with wild-type Ad5 at a multiplicity of infection of 200 virus particles/cell. **D.** TIF1γ localization performed described as in **A**. **E.** E4-ORF3 localization using an anti-E4-ORF3 primary antibody and TRITC-conjugated secondary antibody. **F.** Merge of panels **D** and **E**. **G.** HeLa cells were infected with wild type Ad5 at a multiplicity of infection of 1000 virus particles/cell and analyzed as in **A**. **H–J.** TIF1γ localization at early times after infection with an E4-ORF3 mutant virus at 200 virus particles/cell. **H.** TIF1γ localization performed as described in **A**. **I.** Ad DBP localization using an anti-DBP primary antibody and TRITC-conjugated secondary antibody. **J.** Merge of panels **H** and **I**. **K–M.** TIF1γ localization at late times after infection with wild-type Ad5 at 200 virus particles/cells performed as described in **D–F**.

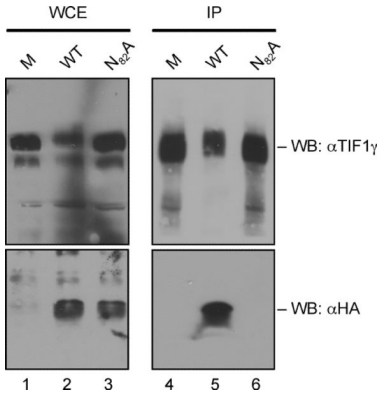

Fig. 2.

The wild-type, but not the N82A mutant, E4-ORF3 protein coimmunoprecipitates with endogenous TIF1γ *in vitro*. HeLa cells were mock-infected (M) or infected with Ad vectors that expressed either the wild-type (WT) or the $N_{82}A$ ($N_{82}A$) mutant HA-tagged E4-ORF3 proteins. Immunoprecipitations from whole cell extracts (WCE) were performed using anti-TIF1γ antibody, and Western blots were probed using antibodies against TIF1γ (top panel) and HA (bottom panel). Lanes 1–3 show proteins present in the starting WCE. Lanes 4–6 show proteins immunoprecipitated with the anti-TIF1γ antibody.

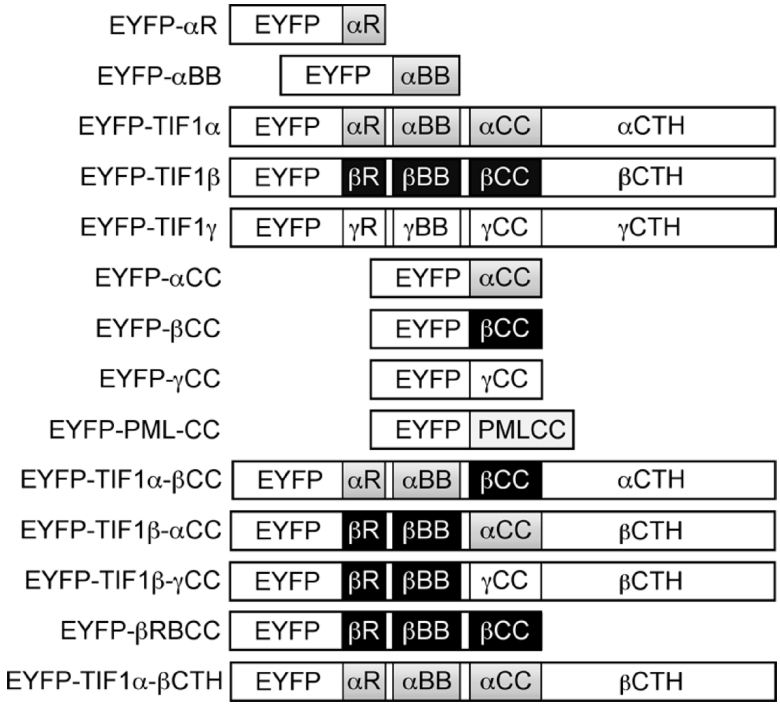

Fig. 3.

Diagram of the EYFP-TIF1 fusion proteins described in the text. Abbreviations are: R, Ring finger domain; BB, B Box domain; CC, Coiled-Coil domain; CTH, C-terminal half; α, TIF1α coding sequences; β, TIF1β coding sequences; γ, TIF1γ coding sequences.

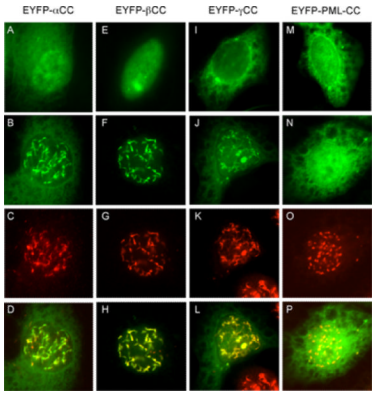

Fig. 4.

E4-ORF3 rearrangement of the Coiled-Coil domains isolated from TRIM family proteins. HeLa cells were transfected with expression vectors encoding EYFP-tagged Coiled-Coil domains from TIF1α (**A–D**), TIF1β (**E–H**), TIF1γ (**I–L**), or PML (**M–P**), then mock-infected (**A, E, I, and M**) or infected with wild-type Ad5 (**F–H, J–L, N–P**). At 18 hours post-infection (**A–L**) or 8 hours post-infection (**M–P**), cells were fixed and stained with an antibody directed against E4-ORF3 followed by a TRITC labeled secondary antibody (**C, G, K, O**). EYFP fusion protein localization is shown in **B**, **F**, **J**, and **N**. EYFP:E4-ORF3 merged images are shown in **D**, **H**, **L**, and **P**.

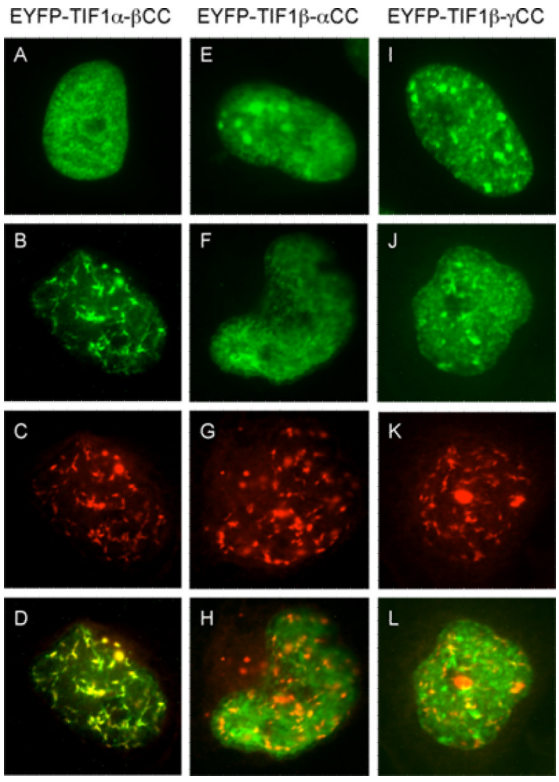

Fig. 5.

E4-ORF3 interaction with the TIF1 Coiled-Coil domain in different protein contexts. HeLa cells were transfected with expression vectors containing EYFP fused to TIF1α containing the Coiled-Coil domain of TIF1β (**A–D**), or TIF1β containing the Coiled-Coil domain of TIF1α (**E–H**) or TIF1γ (**I–L**). Cells were mock-infected (**A, E, I**) or infected with wild-type Ad5 (**B–D, F-H, J–L**). Eighteen hours later, the cells were fixed and stained with an antibody directed against E4-ORF3 followed by a TRITC labeled secondary antibody (**C, G, K**). EYFP fusion protein localization is shown in **A–B, E–F, I–J**. EYFP:E4-ORF3 merged images are shown in **D**, **H**, and **L**.

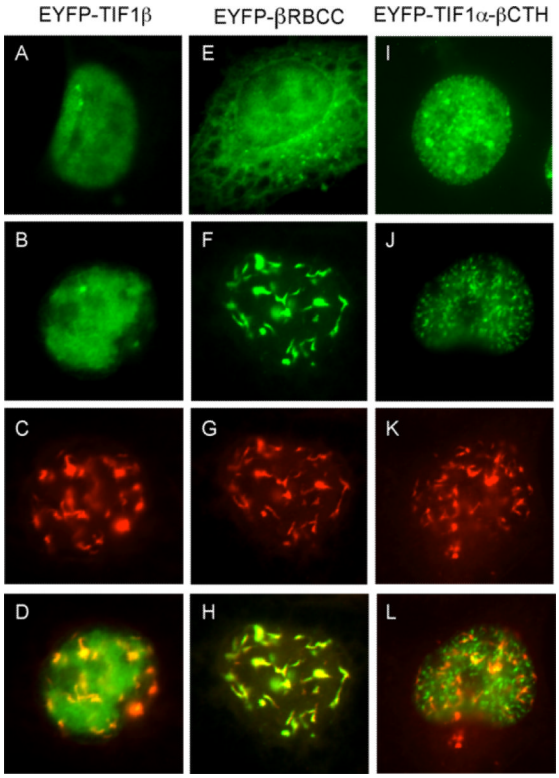

Fig. 6.

The C-terminal half of TIF1β interferes with E4-ORF3-directed TIF1 relocalization. Hela cells were transfected with expression vectors containing EYFP-TIF1β (**A–D**), EYFP-βRBCC (**E-H**), or EYFP-TIF1α-βCTH (**I–J**). Cells were mock-infected (**A, E, I**) or infected with wild-type Ad5 (**B–D, F–G, J–L**). Eighteen hours later, the cells were fixed and stained with an antibody directed against E4-ORF3 followed by a TRITC labeled secondary antibody (**C, G, K**). EYFP fusion protein localization is shown in **A–B, E–F, I–J**. EYFP:E4-ORF3 merged images are shown in **D**, **H**, and **L**.

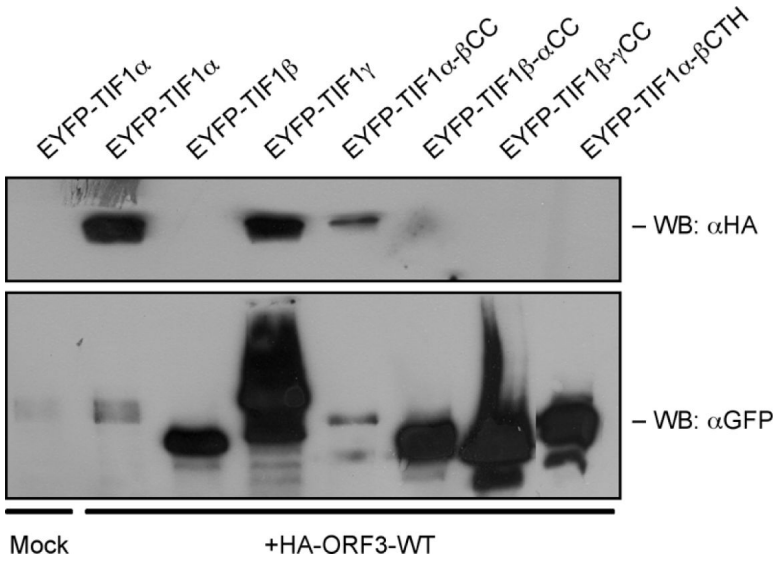

Fig. 7.

Interaction EYFP-TIF1 fusion proteins with wild-type E4-ORF3 *in vitro*. HeLa cells were transfected with expression vectors containing EYFP-TIF1 fusion proteins indicated across the top (see Fig. 3 for depictions) and subsequently mock-infected (Mock, bottom) or infected with an Ad vector expressing HA-tagged wild-type E4-ORF3 protein (+HA-ORF3-WT, bottom). Proteins in cell extracts were immunoprecipitated using an EGFP antibody that cross-reacted with the EYFP and then subject to Western blot analysis using anti-HA (top panel) and anti-GFP (bottom panel) antibodies.

Virology. Author manuscript; available in PMC 2013 January 20.

Table 1

Primer pairs used for PCR.

Primer Set	Construct	5' primer	3' primer	Restriction enzymes
1	EYFP-αRING	GGATCCAGATCTATGGAGGTGGCGGTG	GGATCGCCCGGGTTAGTTCACAAAAAAGTTATCTA	BglII, XmaI
2	EYFP-αBbox	GGATCCAGATCTGACACTACTGAGGTTCC	GGATCCCCCGGGTTAGTATCTATGCTCTTTATGTT	BglII, XmaI
3	EYFP-αCC	GGATCCAGATCTCAATTTATAGAAGAAGCTTTT	GGATCCCCCGGGTTACCTTGCACGAAGGAGG	BglII, XmaI
4	EYFP-βCC	GGATCCAGATCTCAGTTCTTAGAGGATGC	GGATCCCCCGGGTTAAATCATCTTGAGGGCC	BglII, XmaI
5	EYFP-γCC	GGATCCAGATCTCAGTTTTTGGAAGAAGCT	GGATCCCCCGGGTTACCGTGCTTTCAAAATATG	BglII, XmaI
6	EYFP-TIF1α-βCC	GGAAGATCTATCCCCAGTGACCAAC	GGATCCTCTAGATTATTTAAGCAACTGGCGTT	BglII, BamHI, XbaI
7	EYFP-TIF1β-αRBCC	A: GGAAGATCTATGGAGGTGGCGGTG; B: ACCTCCTTAAGATGATTGTGGATCCC	A: CAATCATCTTAAGGAGGTGCCGTAA; B: GGAAGATCTTCAGGGGCCATCACC	BglII
8	EYFP-TIF1β-αRB	GCAAGCTTTTAGGAACCAGCGCAAG	GGAAGATCTTCAGGGGCCATCACC	BglII, BamHI, HindIII
9	EYFP-TIF1β-αCC	GGACTCAGATCTCGAG	GGATCCAAGCTTCCTCTAAGAACTGGTAC	BglII, HindIII
10	EYFP-TIF1β-γCC	TTTTGGAAGAAGCTTTTC	CGCGGATCCCACCGTGCTTTCAAAAT	HindIII, BamHI
11	EYFP-PMLCC	GGAAGATCTTGCGACATCAGCGCA	GGATCCCCCGGGTTACTCCTGGCGCAGGC	BglII, XmaI
12	EYFP-βRBCC	GGACTCAGATCTCGAG	GGATCCGAATTCTTAAATCATCTTGAGGGCC	BglII, BamHI